ISSN 1392–1320 MATERIALS SCIENCE (MEDŽIAGOTYRA). Vol. 21, No. 2. 2015

Improving Hardness of Ni-Cr-Si-B-Fe-C Thermal Sprayed Coatings through Grain Refinement by Vibratory Treatment during Refusion

Jelena ŠKAMAT *, Olegas ČERNAŠĖJUS, Algirdas Vaclovas VALIULIS, Raimonda LUKAUSKAITĖ, Nikolaj VIŠNIAKOV

Vilnius Gediminas Technical University, J. Basanavičiaus 28, LT-03224 Vilnius, Lithuania

crossref http://dx.doi.org/10.5755/j01.mm.21.2.6833

Received 01 April 2014; accepted 11 June 2014

The paper presents studies of vibratory treatment effect on the microstructure and hardness of thermally sprayed and re-fused Ni-based coatings. Ni-Cr-B-Si-Fe-C system powder has been deposited on the S235 steel substrate and re-melted with the simultaneous introduction of the horizontal mechanical vibrations of frequency from 50 Hz to 400 Hz and of amplitude from 25 μm to 185 μm. The microstructure of obtained coatings has been studied along with the microhardness. The grain refinement effect accompanied by the hardness increase up to 20 % has been obtained in vibrated coatings, and frequency from 100 Hz to 200 Hz has been established as the range of the most intensive effect. No visible influence of vibratory treatment on the phase composition has been established.
Keywords: thermal spray, Ni-Cr-B-Si-Fe-C coating, vibratory treatment, microstructure, hardness.

1. INTRODUCTION

The coatings of system Ni-Cr-B-Si-Fe-C, same as the other coatings based on the Ni-Cr-B-Si alloy, are most widely used in a condition when corrosion and oxidation resistance at low and elevated temperatures is required along with the good wear resistance or antifriction features. Boron and silicon provide good self-fluxing characteristics allowing successful re-fusing in air and, normally, such re-fusible coatings are produced by thermal spray process combined with simultaneous or subsequent re-fusing of as-sprayed layer. The two-step spray fuse process has been developed to improve the strength of bond between coating and substrate, and at the same time take advantage of the typical smoothness and uniformity of the coating [1]. The coating features are mainly determined by the structure obtained after layer solidification from the liquid or semi-liquid state reaching by heating the as-sprayed layer during re-fuse step. Thus, an introduction of some optimization and modification of structure may lead to significant improving of the coating performance and quality.

Desirable changes in coatings structure and, respectively, in their properties may be reached in various ways. The change of chemical composition of a spraying powder enables varying the final properties of Ni-based coatings in a wide range from the soft (~300 HV) antifriction coatings with excellent corrosion resistance to the hard (~780 HV) with good wear and erosion resistance. The increased wear resistance is obtainable by addition of high-melting-point and high-hardness compounds such as carbides, nitrides, borides into the coatings [2 – 6]. The rare earth elements have a more complex influence on the properties of the coatings and make a compromise between hardness and toughness besides improving the corrosion and oxidation resistance of the coatings [7 – 10]. The application of different deposition and re-fuse methods normally leads to the partial change in the phase composition and morphology of layers [11 – 15].

At the same time number of researches in the other fields of metallurgy, such as casting and welding, show that the use of specific natures' energies can be effective in control of the metals solidification processes. Thus, the complex positive impact of the low frequency vibrations on the microstructure and properties of ingots have been reported in a lot of works [16 – 21], beginning from 1960's when metal casting under vibrations has been patented for the first time [22, 23]. The melt agitation by vibration energy during solidification causes the breaking of the growing crystals. Thus, the size of growing crystals is limited and broken crystals fragments play the role of new nucleation centers [21]. In results, more homogeneous fine microstructure with the decreased amount of porosity and other defects and with the improved mechanical and special properties tends to be obtained when the vibrations of suitable parameters are introduced during the solidification. There are several other techniques of solidification control: rapid cooling, adding inoculant, employing ultrasound and electric discharge, electromagnetic stirring a. o. [24]. Most of them are associated with high cost, limited applicability for coated large-size components and some other disadvantages from a point of view of the use for protective coatings. At the same time complex positive effect along with the low cost, high efficiency, simple process and no contamination [25] give to vibratory treatment an advantage over the named methods. In technologies of protective metal coatings the effects of vibratory energy have not been studied adequately. A few related publications on laser cladded and plasma sprayed Fe-base coatings have been appeared [25, 26]. The reported results testify the efficiency of the vibratory treatment in the refining of microstructure, improving of the typical features and the uniformity of obtained Fe-based coatings. Three combinations of frequency and amplitude (75 Hz /197 μm; 150 Hz /56 μm

* Corresponding author. Tel.: +370-52-744741; fax: 8-52-745043.
E-mail address: *jelena.skamat@vgtu.lt* (J. Škamat)

and 300 Hz /21 μm) were employed in [26] in two directions – lateral and parallel to the laser cladding direction. The porosity and maximum pore diameter were reduced in all vibrated samples in comparison with unvibrated reference and most powerful lateral vibrations (75 Hz /197 μm) were most effective. The authors indicate also that vibration energy breaks dendrites arms and forms more homogeneous microstructure resulting in less deviation in hardness throughout the buildup. In other work [25] five different frequencies of 50, 75, 100, 125 and 150 Hz were applied under constant amplitude of 90 μm for vibrations, perpendicular to the coating surface. The received results, actually, represent the influence of the increase in frequency, corresponding to the increase in vibrations power, on the microstructure, hardness and wear resistance of the obtained plasma sprayed Fe-based coatings. All the named properties were improved in vibrated coatings and successive increasing of the frequency from 0 Hz to 100 Hz entailed the intensification in grain refinement, hardness increasing and improving of wear resistance. Further increase in frequency was associated to the wane in achieved effects. Thus, the reported results testify the efficiency of the vibratory treatment in refining of microstructure, improving of the typical features and the uniformity of obtained Fe-based coatings. One may assume also that desirable effect of the vibratory treatment is most likely related to the increase in vibration power; however, the effect probably should weaken when some optimal parameters are exceeded.

The lack of the experimental results in the field and absence of any systematization do not allow establishing in what way proper parameters of vibratory treatment may be selected. In the regards to the expedience of application of the vibratory treatment for the Ni-based re-fusible coatings remains an open question also, as there is not enough related data. The present research is aimed at investigating the effect of vibratory treatment on the microstructure and properties of Ni-based coatings in dependence on the parameters of vibrations, what also will supplement new experimental results to the existing database in the field.

It has been shown in earlier published results of the present research [27] that vertical mechanical vibration of the sample during re-fusing step leads to the grain refining accompanied by the increase of the coating hardness when nickel alloy with dominant γ-Ni solid solution solidification is used. Spraying powder of same chemical composition has been used in this part of the work and the influence of horizontal mechanical vibration has been studied.

2. EXPERIMENTAL DETAILS

Commercial self-fluxing Ni-based alloy powder RW12494 from Castolin Eutectic with about 82 % Ni (Table 1) and particle size of 38 μm – 125 μm was used as spraying material. Powder was deposited on structural steel S235 plates of size (100×100×10) mm by oxy-fuel flame spraying. The preparation of substrate and spraying were performed according to recommendation of producer of the powder and spraying/fusing tools (Rototec 80/CastoFuse torch from Castolin Eutectic). The main parameters of process are listed in Table 2. In order to make the same spraying condition for each specimen, robotic equipment Motoman 100 was used. Then as-sprayed layers were re-fused in air by heating up to about 1060 °C with neutral oxy-acetylene flame and cooled in air. Experimental stand for re-fusing under vibratory treatment includes fusing tool (flame torch CastoFuse), gas cylinders of oxygen and acetylene, robot-manipulator Motoman 100 and vibratory equipment – the generator of sinusoidal electric oscillations in the range of 20 Hz – 20 000 Hz, amplifier (3 – 40 000 Hz /50 W /3 Ω) and vibrator converting electric oscillations to mechanical vibrations (VEB RFT Messelektronik Typ 11077, 600 W). Mechanical vibrating of the sample is provided through the rigid mechanical fixing of the sample to the vibrator. Absolute values of the frequency and the amplitude were measured by the set of Machine Diagnostics Toolbox Type 9727 (Bruel & Kjaer), processing the signals coming from the accelerometer fixed directly to the sample under vibrations.

Table 1. Chemical composition of consumed powder (in wt.%)

Ni	Cr	Fe	B	Si	C
bal	10.2	2.79	1.61	3.19	0.44

Table 2. Preparation of substrate and spraying parameters

Preparation of substrate	Cleaning with degreasing agent. Grit blasting, preheating
Spraying flame	Neutral oxy-acetylene
Spraying distance, mm	150
Spraying rate/step/passes	250 mm/s / 5 mm / 8
Average thickness of as-sprayed layer	1.2 mm – 1.3 mm

Table 3. Parameters of vibration condition and samples marking

Frequency, Hz	Amplitude, μm				
	25	50	75	115	185
50	50_25				
75	75_25	75_50	75_75	75_115	75_185
100	100_25	100_50	100_75	100_115	
125	125_25	125_50	125_75		
150	150_25	150_50			
175	175_25				
200	200_25				
250	250_25				
300	300_25				
350	350_25				
400	400_25				

Re-fusing experiments with the application of vibratory treatment were carried out in frequency range from 50 Hz to 400 Hz, selected on the base of the results of primary experiments [27]. Vibrations parameters were chosen on purpose to evaluate the impact of vibration frequency on the coating microstructure as well as the impact of the amplitude. They are listed in Table 3. The minimum of amplitude (25 μm) was selected based on analysis of literature data in the field [16 – 26]: the application of less-intensive amplitude seems to be unreasoned. The maximum amplitude denoted in Table 3 for each employed frequency is the maximum reachable amplitude corresponding to the given frequency for used vibrator. The mechanical vibrations were introduced

parallel to the coating surface, during fusing and after fusing until temperature of the coating reached 500 °C. The series of samples, re-fused without vibratory treatment and marked as A_NV, was used as reference.

Initial powder was investigated by scanning electron microscope (SEM Hitachi SU-70) under magnification of ×200, ×700, and ×1500, and by energy dispersive X-ray microanalysis (EDS). The thermal study of powder was accomplished through differential thermal analysis (DTA), which was carried out with DTA/DSC SETARAM LABSYS equipment. 50 mg of powder was placed in alumina crucible and during non-isothermal experiment was heated in argon (5N) atmosphere from ambient temperature to 1250 °C. The heating rate was 50 °C/min for temperature range from ambient to 750 °C, and 10 °C/min for temperature range from 750 °C to 1250 °C.

The microstructure of sprayed-fused coatings was observed on etched transverse cross-sections using optical microscope Nicon MA 200 and scanning electron microscope SEM Hitachi SU-70. The quantitative evaluation of the grain refining effect has been carried out through the calculation of grain numbers on particular cross-section area of optical micrographs made under ×500 magnification. EDS/WDS analyzers and the necessary software were used in order to perform point microanalysis, linear microanalysis or chemical mapping of the surface under examination.

The phase analysis was done on Philips X-ray powder diffractometer equipped with X-Pert goniometer. Graphite-monochromatized Cu K_α (λ = 0.1541837 nm) radiation was used in all examined cases. Experimental conditions were as follows: voltage valued 40 kV and the current value was 40 mA, angle range 2θ: 20°– 120°, step Δ2θ – 0.032°, exposure time per step – 16 s. The phase structure comparison of vibrated and unvibrated samples was carried out on XRD patterns through comparison of peaks disposition and intensity.

Coatings microhardness measurements have been done by Knoop method using Zwick Roell ZHμ tester with a 1 kg load. Measurements were performed on polished cross-sections, each specimen was measured 10 times and the average values are presented here along with the values of standard deviation. Microhardness measurements of individual phases have been carried out by Vickers method with a 10 g load.

3. RESULTS AND DISCUSSION

After microstructural examination it has been found that consumable powder consists of one-type particles of Ni-based alloy mostly of spherical shape (Fig. 1, a) and having fine crystal structure of primary solidification (Fig. 1, b). The part of powder particles has irregular shape or the shape of coalesced spheres. The particles with so-called satellites can be seen clearly on the micrograph also (Fig. 1, a). During thermal study of powder it was established that the most intensive powders melting correspond to the temperature of 1058 °C. DTA curve is presented on Fig. 2.

After re-melting, coatings microstructure was investigated and specimens, produced under vibratory treatment, were compared with unvibrated reference. XRD pattern of unvibrated coating (A_NV) is presented in Fig. 3 along with the XRD pattern of coating, vibrated with 200 Hz and 25 μm vibrations (A_200_25), which has shown the most intensive grain refinement. Five most intensive peaks may correspond to several different Ni-based phases such as $Cr_{1.12}Ni_{2.88}$, $Cr_{0.1}Ni_{0.9}$, $Ni_{0.98}C_{0.02}$, $FeNi_3$ and $Ni_{2.9}Cr_{0.7}Fe_{0.36}$. Based on the results obtained during further EDS analysis it seems that all the numerous phases are possible. Ni_3B and Cr_7C_3 phases were also established with a high probability. These two phases are most often mentioned in related works [11 – 14, 28 – 33]. The analysis of XRD patterns did not show any visible differences for vibrated and unvibrated coatings.

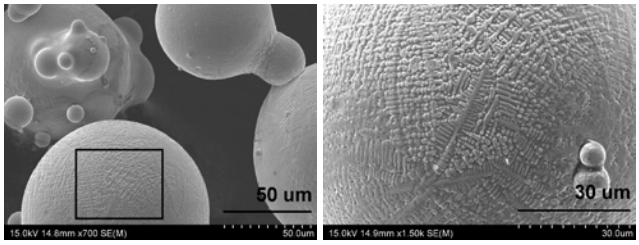

a b

Fig. 1. SEM micrograph of initial powder (a) and denoted area (b)

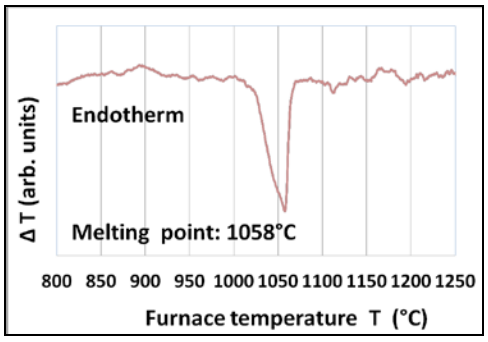

Fig. 2. Endothermic melting peak of Ni-based alloyed powder

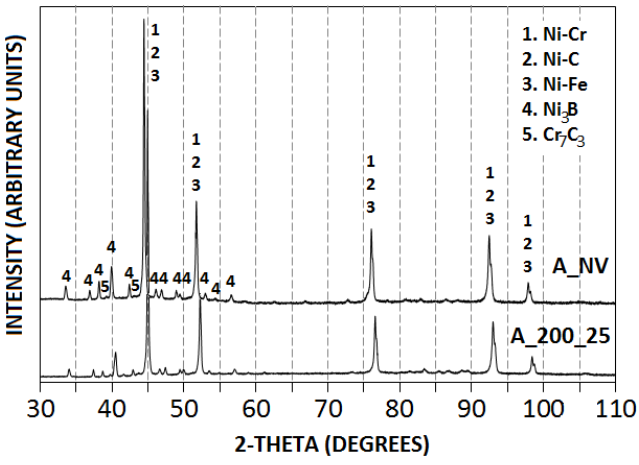

Fig. 3. XRD patterns of unvibrated (A_NV) and vibrated (A_200_25) coatings

The further structure analysis was accomplished using SEM and X-ray microanalysis. Four structural elements, denoted in Fig. 4 as 1, 2, 3 and 4, have been established during microstructure SEM analysis under magnification from ×70 to ×5000. It was found that re-melted coatings microstructure consists of soft metallic 2-phase matrix,

hardened by low amount of hard inclusions of two types at least (Fig. 4, b). The dominant structural element, denoted in Fig. 4 as 1, has near equal axial grain shape and consists mostly of nickel with some presence of Cr, Si, Fe and C. The average hardness of this phase is about 220 HV0.01. Based on related literature analysis [11 – 14, 28 – 33] these grains may be identified as γ-phase – Ni-based solid solution. The areas between γ-Ni grains, denoted in Fig. 4 as 2, contain significant amount of boron besides nickel and, most likely, present Ni/Ni_3B eutectic, reported also by most of other researchers. Hardness values of interdendritic Ni-B phase are in a range from 342 HV to 1230 HV and can be grouped in two intervals. Lower values (342 HV – 626 HV) fit well with the literature data in the field [34] and most likely correspond to Ni/Ni_3B eutectic. Values of upper interval (1190 HV – 1230 HV) are very close to the hardness of nickel boride Ni_3B (1190 HV) [35]. It may indicate that individual Ni_3B particles have formed between γ-Ni grains along with Ni/Ni_3B eutectic.

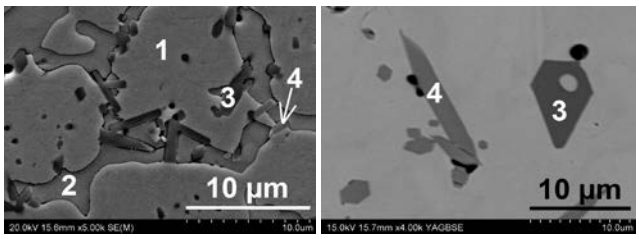

a b

Fig. 4. SEM micrographs of typical microstructure of the coating after etching (a, SE image) and after polishing (b, BSE image): 1 – γ-Ni phase; 2 – Ni-B phase; 3 – carbide phase with higher carbon content; 4 – carbide phase with lower carbon content

The hard phase of the microstructure is represented by Cr-based carbides with the hardness ranged from 1031 HV to 1775 HV. EDS analysis showed also presence of nickel (~8 %) in carbide phase with lower carbon content. According to [36] Cr forms carbides of 3 types: $Cr_{23}C_6$ (976 – 1650 kg/mm^2), Cr_7C_3 (1336 – 2200 kg/mm^2) and Cr_3C_2 (1350 – 2280 kg/mm^2). All of the named carbides have been numerously reported as possible in Ni-based coatings. XRD analysis showed presence of Cr_7C_3 in phase composition. Average carbon content determined by EDS for carbides is as follows: 42.6 % (at.) for the carbide phase with higher carbon content and 31.7 % (at.) for the carbide phase with lower carbon content. Considering the fact that the cross-section surfaces have been coated by carbon film before examination with SEM, the actual carbon content may be significantly lower. Therefore, presence of lower carbides $M_{23}C_6$ and Cr_7C_3 seems as the most probable. Based on the results of hardness measurements the carbides, unidentified during XDR, may also be attributed to $M_{23}C_6$ type, since smaller obtained hardness values (about 1030 HV and above) are closest to the values indicated in [36] as corresponding $Cr_{23}C_6$ carbide. Hence, one may assume that microstructure of re-melted coatings consists of metallic 2-phase γ-Ni / Ni/Ni_3B matrix, hardened by low amount of $(Cr,Ni)_{23}C_6$ and Cr_7C_3 carbides.

The same microstructural elements have been found in coatings re-melted under vibratory treatment. Thus, the application of vibrations does not change the structural and phase composition of coatings as well, as the morphology. The main difference, established during comparative examination, regards the size of dominant γ-Ni grains.

Firstly, the grain size in different cross-section areas of the same sample was compared. Figure 5 illustrates the coating microstructure sensitivity to the solidification condition: it can be seen clearly that both unvibrated (Fig. 5, a – c) and vibrated (Fig. 5, d – f) coatings formed significantly fined grains at the edge of the sample, where the coating cooling is faster. The grain size is growing with moving away from the edge to the sample centre, where cooling rate is lower. The same tendency has been established for all examined samples and microstructure of central cross-section parts were used for further comparative examination.

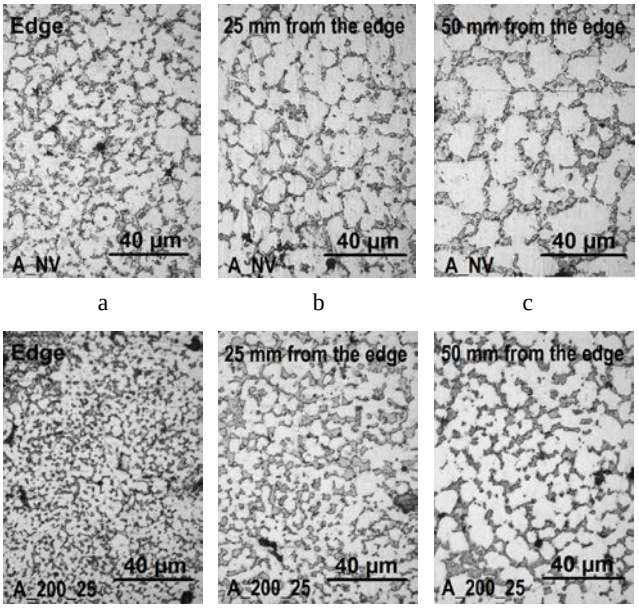

a b c

d e f

Fig. 5. Microstructure of different cross-section zones of unvibrated coating (a – c) and of the coating vibrated under 200 Hz and 25 μm vibrations (d – f): a, d – close to the edge of sample; b, e – about 25 mm from the edge; c, f – at the center of the sample (about 50 mm from the edge)

During examination of the coatings microstructure it was found that grain size in the coating layers, re-melted under vibratory treatment, differs from that in unvibrated coatings and varies with varying of vibrations parameters. Fig. 6 represents microstructures of the coatings with the most refined microstructure (b – f) and with coarse grains (a, g – i). The quantitative evaluation of grain refining effect was carried out through the calculation of grain numbers in particular cross-section area. The coatings microhardness was measured and compared with the average grain numbers. The results are presented in Fig. 7 – 9.

Strong correlation was established between the grain number and the microhardness measurement results: higher microhardness values were obtained on coatings with more refined microstructures. The grains number and the coating microhardness dependences on the vibratory

treatment frequency are presented in Fig. 7. The first diagram shown in Fig. 7 contains the most complete sequence of 12 sample series and hence stays as the most informative diagram for evaluation of a frequency influence. This diagram shows that the increase of grain number accompanied by an increase of microhardness appears periodically. Three peaks corresponding to 50, 125 and 200 Hz and located with an interval of 75 Hz was detected when vibratory treatment of 50 Hz – 400 Hz frequency was applied under constant amplitude of 25 μm. The intensity of peaks rises with an increase of the frequency. Series of specimens, re-melted under the vibration with parameters of 200 Hz and 25 μm, shows the highest microhardness of 372 HK (~20 % more than of the unvibrated series) and the most refined structure. The average grain number (AGN) in 25000 μm^2 area was 334 for these coatings. This value ~2.4 times exceeds AGN for the unvibrated coatings.

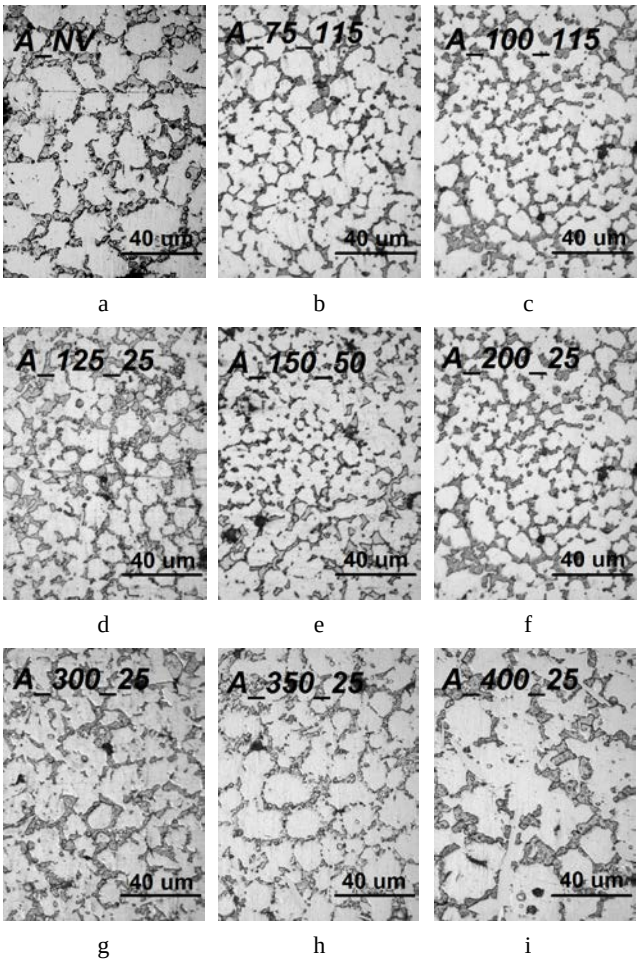

a b c d e f g h i

Fig. 6. Microstructure of central cross-section zone (about 50 mm from the edge) of unvibrated coating (a) and of the coatings vibrated under various parameters (b – i)

The microstructure of coatings re-melted under vibrations with parameters of 350 Hz /25 μm and 400 Hz /25 μm, by contrast, showed slight increase in grain size and corresponding downturn of hardness below that of unvibrated reference. Some increase in grain size caused by vibratory treatment is reported in [37] also. Convection modifying to conditions, when the amount of spontaneous crystallization nucleus is limited, is reported in [37] as possible. In present research the solidification of remelted layers starts from the interface, where the substrate acts as a heat sink. Coarse grains in vibrated coatings may indicate some disturbance in the interaction between the substrate and the coating due to vibration energy, what affects heat transfer through the interface. Thus, availability of both grain refinement and grain growth in vibrated layers may testify that vibrations influence the solidification process in different rival ways and the dominance of one over others is related to the parameters of vibrations.

The rest diagrams presented in Fig. 7 contain shorter sequences of 3 – 5 sample series and do not allow establishing the regularity in varying of the microhardness and AGN. It's noticeable also that the 3rd diagram is in a certain compliance with the results of work [25]: the amplitude of 75 μm was close to that from work [25] – 90 μm and, same as in [25], showed the most intensive effect under the frequency of 100 Hz with further wane of effect under increasing of frequency.

Dependences of grain numbers and the coatings microhardness on the vibratory treatment amplitude are presented in Fig. 8. It was found that every sequence corresponding to a definite frequency contains certain amplitude corresponding to the most intensive effects. Close values of AGN and microhardness have been determined on samples vibrated under different vibrations parameters (75 Hz /115 μm, 100 Hz /115 μm, 125 Hz / 25 μm, 150 Hz /50 μm), what indicates that similar effect may be reached when various frequency and amplitude combinations are applied.

After the most effective amplitude was selected from each frequency series, corresponding AGN values along with the microhardness were set in order of frequency increasing. Obtained diagram is presented in Fig. 9. Based on this diagram one can summarize that for the vibrations parameters investigated in this work the range of most intensive grain refining and microhardness increasing effects may be determined as 100 Hz – 200 Hz.

AGN values obtained on the coatings vibrated with 100 Hz – 200 Hz frequency were from 301 to 344. These values 2.2 – 2.4 times exceed AGN for the unvibrated reference (137 grains /25000 μm^2). The microhardness values were from 339 HK to 372 HK for these coatings and this exceeds by 9 % – 20 % than of those unvibrated references. It should be noted also that the results obtained under combination of higher frequency with smaller amplitude (150_50, 200_200) are similar to those obtained under smaller frequency and higher amplitude (75_115, 100_115). This testifies that level of vibrations power may be the dominant complex parameter of vibratory treatment instead of individual parameters – frequency or amplitude. On the other hand, no certain dependence “effect-from-power” was determined at the moment and further research is required in the field.

The amplitude sequences, presented in Fig. 8, contain only 3 – 6 series, despite that, the peak has appeared in each diagram. Therefore, from the point of view of parameters selection, amplitude seems more convenient parameter. The most intensive applied amplitudes, listed in Table 3, were limited by the used equipment in this work. Authors believe that further increase of the amplitude may lead to some additional reinforcement of the obtained effect and the further research is expedient in the field.

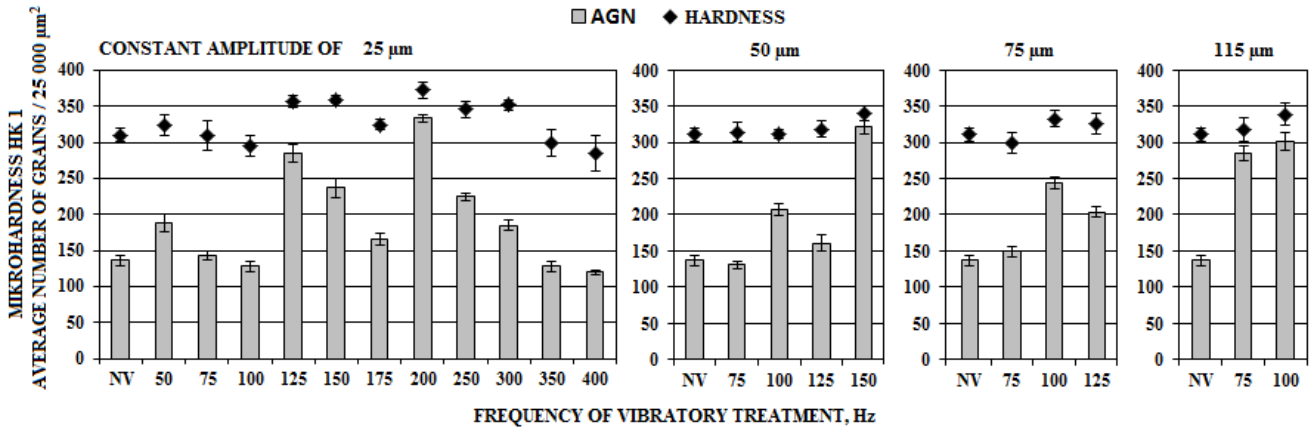

Fig. 7. Coatings Knoope microhardness (HK 1), measured parallel to the substrate, and average grains number (AGN) in dependence on frequency increasing under constant amplitudes of 25, 50, 75 and 115 µm

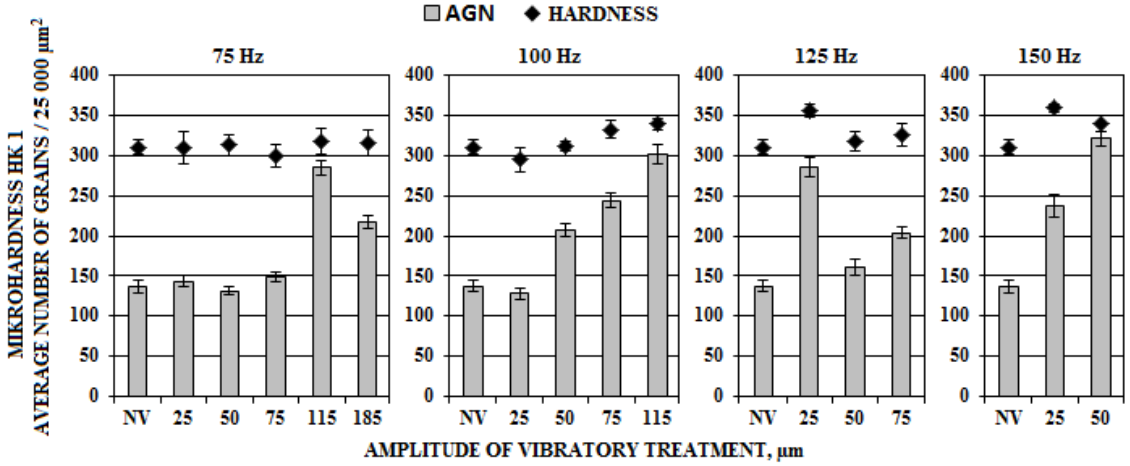

Fig. 8. Coatings Knoope microhardness (HK 1), measured parallel to the substrate, and average grains number (AGN) in dependence on amplitude increasing under constant frequencies of 75, 100, 125 and 150 Hz

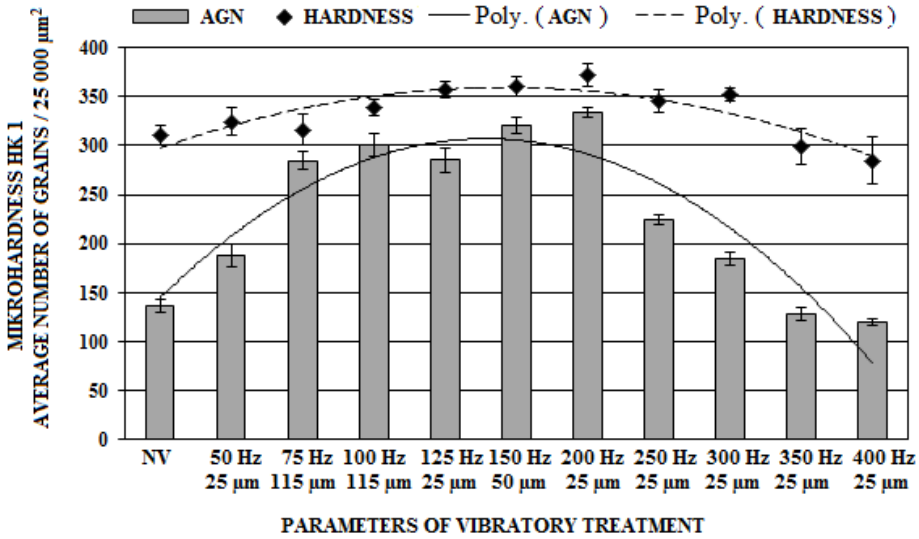

Fig. 9. The biggest values of coatings Knoope microhardness (HK 1) measured parallel to the substrate and average grain number (AGN), selected from each frequency series, in order of frequency increasing

4. CONCLUSIONS

The application of horizontal mechanical vibrations during re-melting of as-sprayed Ni-based coatings influences their final microstructure, namely – grain refinement effect accompanied by an increase of coating hardness may be obtained when vibrations of certain parameters are used for alloy with dominant solidification of γ-Ni phase. Therefore, one may summarize, that a coating wear resistance and its durability should improve.

Strong correlation between results of microstructural analysis and hardness measurements along with the absence of any visible phase composition difference for vibrated and unvibrated coatings allows assuming that obtained hardness increase is reached mostly due to the grain refinement.

The presented research covers the investigation of the vibratory treatment ranged from 50 Hz to 400 Hz and the most intensive effects have been found in the range from 100 Hz to 200 Hz. The highest AGN value (334 grains/ /25000 μm^2) corresponds to the coatings obtained by vibration of 25 μm amplitude and 200 Hz frequency. This value ~2.4 times exceeds AGN for the unvibrated reference and corresponds to ~20 % increase in the coating microhardness.

REFERENCES

1. **Grainger, S., Blunt, J.** Engineering Coatings – Design and Application. Second Edition. Abington Publishing, Cambridge, 1998: 336 p. http://dx.doi.org/10.1533/9781845698577
2. **Cai, B., Tan, Y., He, L., Tan, H., Gao, L.** Tribological Properties of TiC Particles Reinforced Ni-based Alloy Composite Coatings *Transactions of Nonferrous Metals Society of China* 23 (6) 2013: pp. 1681 – 1688. http://www.sciencedirect.com/science/article/pii/S1003632613626485 http://dx.doi.org/10.1016/S1003-6326(13)62648-5
3. **Chen, H., Xu, C., Chen, J., Zhao, H., Zhang, L., Wang, Z**. Microstructure and Phase Transformation of WC/Ni60B Laser Cladding Coatings During Dry Sliding Wear *Wear* 264 (7 – 8) 2008: pp. 487 – 493. http://www.sciencedirect.com/science/article/pii/S0043164807006400
4. **Li, Q., Songb, G. M., Zhang, Y. Z., Lei, T. C., Chena, W. Z.** Microstructure and Dry Sliding Wear Behavior of Laser Clad Ni-based Alloy Coating with the Addition of SiC *Wear* 254 (3 – 4) 2003: pp. 222 – 229. http://www.sciencedirect.com/science/article/pii/S0043164803000073
5. **Niranatlumpong, P., Koiprasert, H.** Phase Transformation of NiCrBSi-WC and NiBSi-WC arc Sprayed Coatings *Surface and Coatings Technology* 206 (2 – 3) 2011: pp. 440 – 445. http://www.sciencedirect.com/science/article/pii/S0257897211007493
6. **Wu, P., Du, H. M., Chen, X. L., Li, Z. Q., Bai, H. L., Jiang, E. Y.** Influence of WC Particle Behavior on the Wear Resistance Properties of Ni–WC Composite Coatings *Wear* 257 (1 – 2) 2004: pp. 142 – 147. http://www.sciencedirect.com/science/article/pii/S0043164803006124
7. **Sharma, S.** Wear Study of Ni-WC Composite Coating Modified with CeO_2 *International Journal of Advanced Manufacturing Technology* 61 (9 – 12) 2012: pp. 889 – 900. http://link.springer.com/article/10.1007%2Fs00170-011-3764-x#page-1
8. **Sharma, S. P., Dwivedi, D. K., Jain, P. K.** Effect of La_2O_3 Addition on the Microstructure, Hardness and Abrasive Wear Behaviour of Flame Sprayed Ni Based Coatings *Wear* 267 (5 – 8) 2009: pp. 853 – 859. http://www.sciencedirect.com/science/article/pii/S0043164809000180
9. **Zhang, Z., Wang, Z., Liang, B., Dong, H. B., Hainsworth, S. V.** Effect of CeO_2 on the Microstructure and Behaviour of Thermal Spray Welded NiCrWRe Coatings *Wear* 262 (5 – 6) 2007: pp. 562 – 567. http://www.sciencedirect.com/science/article/pii/S0043164806002912
10. **Zhang, Z., Lu, X., Han, B., Luo, J.** Rare Earth Effect on the Microstructure and Wear Resistance of Ni-based Coatings *Materials Science and Engineering* A 454 – 455 2007: pp. 194–202.
11. **Gonzalez, R., Garcia, M. A., Penuelas, I., Cadenas, M., del Rocio Fernandez, Ma., Hernandez Battez, A., Felgueroso, D.** Microstructural Study of NiCrBSi Coatings Obtained by Different Processes *Wear* 263 (1 – 6) 2007: pp. 619 – 624. http://www.sciencedirect.com/science/article/pii/S0043164807004061
12. **Li, Q., Zhang, D., Lei, T., Chen, Ch., Chen, W.** Comparison of Laser-clad and Furnace-melted Ni-based Alloy Microstructures *Surface and Coatings Technology* 137 (2 – 3) 2001: pp. 122 – 135. http://www.sciencedirect.com/science/article/pii/S0257897200007325
13. **Navas, C., Colaco, R., de Damborenea, J., Vilar, R.** Abrasive Wear Behaviour of Laser Clad and Flame Sprayed-melted NiCrBSi Coatings *Surface and Coatings Technology* 200 (24) 2006: pp. 6854 – 6862. http://www.sciencedirect.com/science/article/pii/S0257897205011254 http://dx.doi.org/10.1016/j.surfcoat.2005.10.032
14. **Serres, N., Hlawka, F., Costil, S., Langlade, C., Machi, F.** Microstructure and Environmental Assessment of Metallic NiCrBSi Coatings Manufactured via Hybrid Plasma Spray Process *Surface and Coatings Technology* 205 (4) 2010: pp. 1039 – 1046. http://www.sciencedirect.com/science/article/pii/S0257897210002513 http://dx.doi.org/10.1016/j.surfcoat.2010.03.048
15. **Xu, G., Kutsuna, M., Liu, Z., Zhang, H.** Characteristics of Ni-based Coating Layer Formed by Laser and Plasma Cladding Processes *Materials Science and Engineering* A 417 (1 – 2) 2006: pp. 63 – 72. http://www.sciencedirect.com/science/article/pii/S092150930501049X
16. **Chirita, G., Stefanescu, I., Soares, D., Silva, F. S**. Influence of Vibration on the Solidification Behavior and Tensile Properties of an Al-18 wt% Si Alloy *Materials and Design* 30 (5) 2009: pp. 1575 – 1580. http://dx.doi.org/10.1016/j.matdes.2008.07.045
17. **Limmaneevichitr, Ch., Pongananpanya, S., Kajornchaiyakul, J.** Metallurgical Structure of A356 Aluminum Alloy Solidified under Mechanical Vibration: An Investigation of Alternative Semi-solid Casting Routes *Materials and Design* 30 (9) 2009: pp. 3925 – 3930.

18. **Nuradinov, A. S.** Control of Formation Structure of Metal Billets by Heatforce Influences on Solidifying Alloys. Thesis for Competition for Doctor of Engineering Science. Kiev, 2007.
19. **Sulitsin, A. V., Mysik, R. K., Golodnov, A. I., Brusnitsin, S. V.** Vibration Influence on the Inverted-V-shaped and Dendritic Segregation of Cadmium in Ingots of Cadmium Bronze *Metallurgy and Materials Technology* IV – 1 (4) 2010: pp. 47 – 53.
20. **Taghavi, F., Saghafian, H., Kharrazi, Y. H. K.** Study on the Effect of Prolonged Mechanical Vibration on the Grain Refinement and Density of A356 Aluminum Alloy *Materials and Design* 30 (5) 2009: pp. 1604 – 1611. http://dx.doi.org/10.1016/j.matdes.2008.07.032
21. **Wu, S., Xie, L., Zhao, J., Nakae, H.** Formation of Non-dendritic Microstructure of Semi-solid Aluminum Alloy under Vibration *Scripta Materialia* 58 (7) 2008: pp. 556 – 559. http://dx.doi.org/10.1016/j.scriptamat.2007.11.010
22. **Ornitz, N.** Metal Casting. US patent No. 2897557, 1959.
23. **Patton, A.** Metal Casting. US patent No. 3045302, 1962.
24. **Kudrin, V.** Out-of-furnace Processing of Cast Iron and Steel. Metallurgy, Moscow, 1992: 336 p.
25. **Wang, S., Li, H., Chen, X., Chi, J., Li, M., Chai, L., Xu, H.** Improving Microstructure and Wear Resistance of Plasma Clad Fe-based Alloy Coating by a Mechanical Vibration Technique during Cladding *Materials Science and Engineering* A 528 2010: pp. 397 – 401. http://www.sciencedirect.com/science/article/pii/S0921509310010518 http://dx.doi.org/10.1016/j.msea.2010.09.021
26. **Foroozmehr, E., Lin, D., Kovacevic, R.** Application of Vibration in the Laser Powder Deposition Process *Journal of Manufacturing Process* 11 (1) 2009: pp. 38 – 44. http://www.sciencedirect.com/science/article/pii/S1526612509000395
27. **Škamat, J., Valiulis, A. V., Černašėjus, O.** The Influence of Mechanical Vibrations on Properties of Ni-based Coatings *Journal of Vibroengineering* 12 (4) 2010: pp. 604 – 610.
28. **Lebaili, S., Durand-Charre, M., Hamar-Thibault, S.** The Metallurgical Structure of As-solidified Ni-Cr-B-Si-C Hardfacing Alloys *Journal of Materials Science* 23 1988: pp. 3603 – 3611. http://dx.doi.org/10.1007/BF00540502
29. **Kim, H.-J., Hwang, S.-Y., Lee, Ch.-H., Juvanon, P.** Assessment of Wear Performance of Flame Sprayed and Fused Ni-based Coatings *Surface and Coating Technology* 172 2003: pp. 262 – 269.
30. **Hemmati, I., Ocelik, V., De Hosson, J. T. M**. Effects of the Alloy Composition on Phase Constitution and Properties of Laser Deposited Ni-Cr-B-Si Coatings *Physics Procedia* 41 2013: pp. 302 – 311. http://www.sciencedirect.com/science/article/pii/S1875389213000965 http://dx.doi.org/10.1016/j.phpro.2013.03.082
31. **Hou, Q. Y., Huang, Z. Y., Shi, N., Gao, J. S.** Effects of Molybdenum on the Microstructure and Wear Resistance of Nickel-based Hardfacing Alloys Investigated Using Rietveld Method *Journal of Materials Processing Technology* 209 (6) 2009: pp. 2767 – 2772.
32. **Shrestha, S., Hodgkiess, T., Neville, A.** Erosion-corrosion Behaviour of High-velocity Oxy-fuel Ni-Cr-Mo-Si-B Coatings under High-velocity Seawater Jet Impingement *Wear* 259 (1 – 6) 2005: pp. 208 – 218.
33. **Sudha, C., Shankar, P., Subba Rao, R. V., Thirumurugesan, R., Vijayalakshmi, M., Baldev Raj.** Microchemical and Microstructural Studies in PTA Weld Overlay of Ni-Cr-Si-B Alloy on AISI 304L Stainless Steel *Surface and Coatings Technology* 202 (10) 2008: pp. 2103 – 2112. http://dx.doi.org/10.1016/j.surfcoat.2007.08.063
34. **Liyanage, T., Fisher, G., Gerlich, A. P.** Influence of Alloy Chemistry on Microstructure and Properties in NiCrBSi Overlay Coatings Deposited by Plasma Transferred arc Welding (PTAW) *Surface and Coatings Technology* 205 (3) 2010: pp. 759 – 765. http://dx.doi.org/10.1016/j.surfcoat.2010.07.095
35. **Sobolev, A., Fedorov, T.** Phase Diagram of the System Nickel-boron. Academy of Science, Moscow, Inorganic Materials 3 (4) 1967: 723 p.
36. **Chattopadhyay, R.** Surface Wear – Analysis, Treatment, and Prevention. USA, ASM International, 2001: 307 p.
37. **Jurčius, A.** Effect of Vibratory Treatment on Residual Stresses in Structural Steel Weldments. Doctoral Dissertation. Vilnius: 2010.